Available online at www.sciencedirect.com
ScienceDirect
Optics Communications 281 (2008) 2265–2270
OPTICS COMMUNICATIONS
www.elsevier.com/locate/optcom

Compact low threshold Cr:YAG passively Q-switched intracavity optical parametric oscillator

Jieguang Miao [a,b,*], Jiying Peng [a,b], Baoshan Wang [a,b], Huiming Tan [a], Huikun Bian [a,b]

[a] *Changchun Institute of Optics, Fine Mechanics and Physics, Chinese Academy of Sciences, Changchun, Jilin 130033, China*
[b] *Graduate School of Chinese Academy of Sciences, Beijing 100039, China*

Received 12 December 2006; received in revised form 30 September 2007; accepted 4 December 2007

Abstract

We report a compact KTP-based intracavity optical parametric oscillator (IOPO) driven by a diode-end-pumped passively Q-switched Nd:YVO_4/Cr:YAG laser. For the first time, we take the thermal lens effect of the Cr:YAG into consideration and discuss its impact on the signal output. Diode pump threshold as low as 0.52 W has been achieved, which is the lowest result reported to date. At the incident diode pump power of 4 W, we obtained the maximum signal average and peak power of 358 mW and 12.5 kW, respectively, corresponding to a diode-to-signal conversion efficiency of 9%. Moreover, cavity-dumping characteristic and pulse transforming process from 1064 to 1573 nm are qualitatively analyzed.

PACS: 42.65.Yj; 42.55.Xi; 42.60.Gd

Keywords: Optical parametric oscillator; Passively Q-switching; Diode-pumped lasers; Thermal lens

1. Introduction

During the past decades, all-solid-state optical parametric oscillators (OPOs) have attracted particular research interests. Differing from common lasers, OPO gain is provided through the energy coupling process in the nonlinear medium. In other words, the incident pump energy, under the action of the second-order nonlinear polarization, is coupled into the signal and idler fields. Therefore, nonlinearity of the OPO crystal is a vital factor to increase the parametric gain and lower the OPO oscillation threshold. Besides, pump intensity is another key factor that affects the OPO efficiency. Generally, in order to increase the pump intensity, we have to either employ high energy side-pumped pulsed lasers as the pump sources, or to focus the pump beam as tightly as possible. However, some corresponding problems inevitably arise, such as bulky and complicated configuration, optical damage, increased walk-off, etc.

To overcome the issues mentioned above, an alternative approach is intracavity OPO (IOPO). Taking advantage of the high intracavity pump intensity, IOPO decreases the pump level necessary to reach the OPO threshold and increases the overall efficiency. Since the early 1990s, IOPO has gained a renaissance after about 20 years dreariness. Nevertheless, the pump sources mainly are flash-lamp side-pumped or quasi-cw-diode-end-pumped actively Q-switched Nd:YAG lasers [1,2] with low pulse repetition rate and low overall efficiency. In recent years, diode (cw)-end-pumped solid-state Cr:YAG passively Q-switched lasers, with the virtue of low cost, high efficiency, compactness and simplicity [3,4], have attracted much attention and become an alternative to actively Q-switched lasers. The first IOPO driven by a diode-end-pumped Q-switched Nd:YVO_4 laser was realized by Conroy et al. [5]. Lately,

* Corresponding author. Address: Changchun Institute of Optics, Fine Mechanics and Physics, Chinese Academy of Sciences, Changchun, Jilin 130033, China.
E-mail address: mjgbhk@yahoo.com (J. Miao).

0030-4018/$ - see front matter © 2007 Elsevier B.V. All rights reserved.
doi:10.1016/j.optcom.2007.12.012

Chen et al. [6,7] and Zendzian et al. [8] demonstrated several such IOPOs with diode pump thresholds over 1.1 W and diode-to-signal conversion efficiencies higher than 10%. However, to our knowledge, no previous discussion was carried out on the thermal lens effect of the Cr:YAG saturable absorber, which we consider very important for high power signal output.

Recently, we demonstrated a small scale diode-end-pumped actively Q-switched eye-safe IOPO with diode pump threshold as low as 0.86 W [9]. In this letter, we report a diode-end-pumped Cr:YAG passively Q-switched IOPO emitting at 1573 nm. A much lower diode pump threshold of 0.52 W has been obtained, and it is confirmed to be lower than any other previously published results. In addition, for the first time, we take the thermal lens effect of the Cr:YAG into consideration and discuss its impact on the signal output.

2. Experimental setup

The experimental configuration of the IOPO is schematically shown in Fig. 1a. A passively Q-switched $Nd:YVO_4$/Cr:YAG laser, longitudinally driven by a 5 W cw diode laser (806.5 nm, Lasertel LT-1030), was employed as the pump source of the OPO. Owing to the divergent and unsymmetrical emitting properties of the diode, a well designed coupling optics was used here with a coupling efficiency of 93%. In order to reduce the OPO threshold, a plane-concave cavity configuration was used in this setup to set the fundamental beam waist near the KTP crystal. As an input mirror, M1 was anti-reflection (AR) coated at 808 nm on both sides and high-reflection (HR) coated at 1064 nm on the concave one with a radius of curvature of 50 mm. Taking advantages of high absorption cross section and linearly polarized emitting characteristic, a $3 \times 3 \times 5\ mm^3$, a-cut, 0.5 at.% doped $Nd:YVO_4$ was used as the active medium which was AR coated at 1064 nm on both sides. Several Cr:YAG saturable absorbers with three different thickness and initial transmission of 2.65, 3.35, 1.80 mm and 60%, 70%, 83%, respectively, were used here to study their impact on the signal output. The KTP crystal, with a length of 20 mm and cut for type-II non-critical phase-matching ($\theta = 90°$, $\phi = 0°$), was used as the nonlinear parametric converter. In order to reduce the inserting loss, one side of the KTP was coated as one of the OPO cavity mirrors, which was high-transmission at 1064 nm ($T > 95\%$) and HR at 1573 nm ($R > 99.8\%$), and was AR coated at both 1064 and 1573 nm on the other side. Serving as the cavity mirror for both the fundamental and OPO cavities, M2 was HR coated at 1064 nm ($R > 99.8\%$) and partly-reflection coated at 1573 nm ($R = 86\%$) on one side, and was AR coated at the two waves on the other side. Moreover, several thermo-electric coolers were used in the experiment to thermally stabilize the laser rod, Cr:YAG and KTP crystals.

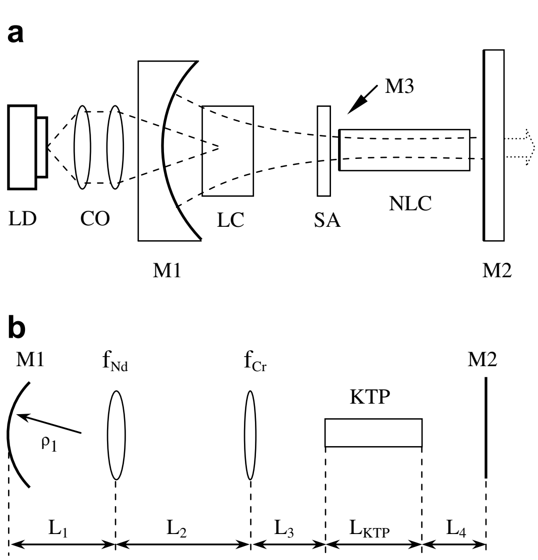

Fig. 1. (a) Experimental setup of the IOPO system. LD, laser diode. CO, coupling optics. M1, input mirror. LC, laser crystal. SA, Cr:YAG saturable absorber. NLC, KTP crystal. M2, output coupler. (b) Equivalent cavity of the KTP-based IOPO with two thermal lenses.

3. Thermal lens discussion

Thermal lens effect (TLE) is always an obstacle to stable, efficient and high power laser output with good beam quality [10,11]. So, it is a vital factor in the design and optimization of all-solid-state lasers. Among all the parameters that contribute to the TLE, as described in Eq. (1), pump intensity is the most important one. Thus, we note that the TLE would also be very serious even at moderate or low output level if the pump beam waist is very small, resulting in high pump intensity. Most of the former works were focused on the TLE in the active medium, and the lasers mainly operated in the continuous wave (cw) regime. Recently, Song et al. [12] treated the TLE of the Cr:YAG saturable absorber as an important factor in high power passively Q-switched lasers. In this work, we first introduce it into a passively Q-switched IOPO system and discuss its impact on the signal output.

The most widely used formula to estimate the thermal focal length was first reported by Innocenzi et al. as follows [13]

$$f = \frac{K_c}{\xi I_{in}(dn/dT)} \cdot \frac{1}{1 - \exp(-\alpha l)} \tag{1}$$

where K_c is the thermal conductivity, α and dn/dT, respectively, are the absorption and thermo-optic coefficients, ξ is the fractional thermal load, l is the crystal length. Besides, the absorbed pump intensity I_{in} can be expressed as

$$I_{in} = \frac{P_{in}}{\pi \omega_p^2} \tag{2}$$

here ω_p and P_{in} are the pump beam waist and absorbed diode pump power, respectively.

Considering the TLE in the Cr:YAG saturable absorber, there are two thermal lenses in the IOPO system. We introduce f_{Cr} and f_{Nd} to describe the focal lengths in the Cr:YAG and Nd:YVO_4 crystals, respectively. Obviously, f_{Nd} can be directly calculated from Eq. (1). However, owing to the intensity dependent absorption coefficient of the Cr:YAG saturable absorber, the calculation of f_{Cr} seems to be more complicated, and the absorption coefficient is defined by

$$\alpha = \frac{\alpha_0}{1 + I_{in}/I_s} \tag{3}$$

where α_0 is the small-signal absorption coefficient which is related to the initial transmission T_0 as follows

$$\alpha_0 = \frac{1}{l}\ln(1/T_0) \tag{4}$$

and I_s is the saturation intensity given by

$$I_s = hv/\sigma_{gs}\tau_f \tag{5}$$

here hv is the photon energy of the incident light, τ_f and σ_{gs}, respectively, are the excited-state life time and ground-state absorption cross section of Cr:YAG.

In order to theoretically analyze the impact of the two thermal lenses on the OPO output performance, we employed the standard ABCD matrix approach. Fig. 1b depicts the equivalent cavity of the IOPO with two thermal lenses. Based on the ABCD matrix theory, taking M1 as the reference plane, the single-trip transforming matrix of the present cavity configuration can be written as

$$\begin{pmatrix} a & b \\ c & d \end{pmatrix} = \begin{pmatrix} 1 & L_4 \\ 0 & 1 \end{pmatrix}\begin{pmatrix} 1 & 0 \\ 0 & n_{KTP} \end{pmatrix}\begin{pmatrix} 1 & \frac{L_{KTP}}{n_{KTP}} \\ 0 & 1 \end{pmatrix} \times \begin{pmatrix} 1 & 0 \\ 0 & \frac{1}{n_{KTP}} \end{pmatrix}\begin{pmatrix} 1 & L_3 \\ 0 & 1 \end{pmatrix}\begin{pmatrix} 1 & 0 \\ -\frac{1}{f_{Cr}} & 1 \end{pmatrix} \times \begin{pmatrix} 1 & L_2 \\ 0 & 1 \end{pmatrix}\begin{pmatrix} 1 & 0 \\ -\frac{1}{f_{Nd}} & 1 \end{pmatrix}\begin{pmatrix} 1 & L_1 \\ 0 & 1 \end{pmatrix} \tag{6}$$

where L_1, L_2, L_3 and L_4 are the distances among the elements that constitute the cavity, L_{KTP} and n_{KTP}, respectively, are the length and refractive index of the KTP crystal. Furthermore, the equivalent G parameters of the multi-element cavity can be defined by [14]

$$G_1 = a - b/\rho_1, \quad G_2 = d - b/\rho_2 \tag{7}$$

here ρ_1 and ρ_2 are the radii of curvature of the cavity mirrors M1 and M2, respectively. Since M2 is a plane-parallel mirror, the value of ρ_2 is infinite, and the expression of G_2 is consequently simplified as $G_2 = d$. According to the cavity stability condition, the product of G_1 and G_2 should satisfy

$$0 < G_1G_2 < 1 \tag{8}$$

Fig. 2 illustrates the variation of G_1G_2 as a function of the incident diode pump power. The parameters used in this calculation mostly are listed in Table 1. Besides, $n_{KTP} = 1.745$, $\rho_1 = 50$ mm, $L_1 = 2$ mm, $L_2 = 26$ mm, $L_3 = 2.5$ mm, $L_4 = 1.5$ mm. Previous studies revealed that the fractional thermal load (ξ) of Nd-doped crystals mainly depends on the dopant concentration, impurity quenching, nonradiative relaxing, etc. [15,16]. Especially, Lan et al. indicated that ξ also has a dependence on the pulse repetition rate when the lasers operate in the pulsed regime, which essentially is attributed to the effect of energy-transfer upconversion (ETU) [17]. Therefore, taking into account the 0.5 at.% doped Nd:YVO_4 crystal, we assumed $\xi = 0.15$, 0.13 and 0.11 for the OPO operations with $T_0 = 60\%$, 70% and 83%, respectively. On the other hand, considering the ESA effect of the Cr:YAG saturable absorbers, we used $\xi = 0.16$, 0.13 and 0.08, in the calculations of f_{Cr} for the Cr:YAG samples with $T_0 = 60\%$, 70% and 83%, respectively. As shown in Fig. 2, the value of G_1G_2 decreases linearly with the incident diode pump power, indicating that the TLE in the Nd:YVO_4 and Cr:YAG crystals became more and more serious when the pump intensity went higher. In the cases of $T_0 = 70\%$ and 83%, G_1G_2 persistently matches the cavity stability condition on the whole pump scope. However, when the diode pump power went beyond 3.5 W, the parametric operation with $T_0 = 60\%$ switched into the unstable region, which inevitably would lead to the power fall-off and even quenching of the IOPO.

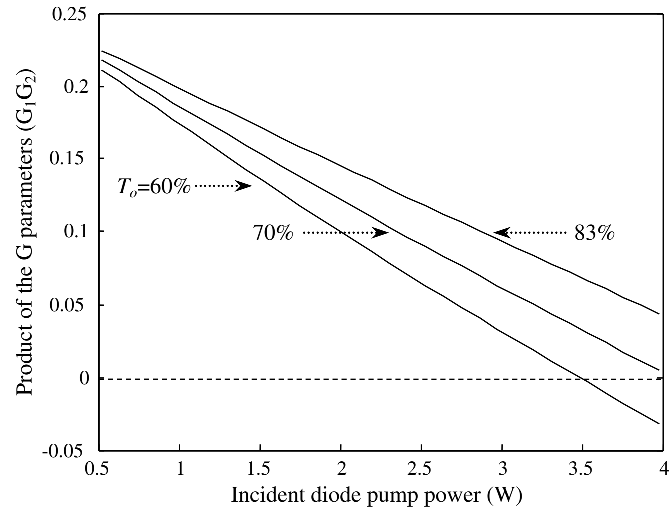

Fig. 2. Variations of the product of G_1 and G_2 with respect to the incident diode pump power, using different Cr:YAG samples.

Table 1
Parameters used in the calculation of the thermal focal length of the passively Q-switched IOPO

Parameters	Cr:YAG	Nd:YVO_4
dn/dT	8.0×10^{-6}/K	$(4.7 \pm 0.6) \times 10^{-6}$/K
K_c	12.1 W/mK	5.4 W/mK
ω_p	130 μm	150 μm
α	/	14.8 cm^{-1}
hv	1.86×10^{-19} J	/
τ_f	3.4 μs	/
σ_{gs}	4.3×10^{-18} cm^2	/

4. Experimental results and discussion

The overall physical cavity length of the IOPO was designed to be approximately 56 mm to optimize the mode-to-pump ratio. In order to enhance the parametric conversion efficiency, *y*-axis of the KTP was placed exactly parallel to the π-polarization direction of the fundamental wave. Fig. 3 shows the average output at 1573 nm as a function of the incident diode pump power for different Cr:YAG saturable absorbers. Diode pump threshold as low as 0.52 W has been achieved, which, to the best of our knowledge, is the lowest result under the similar experimental conditions. It is necessary to mention that the present OPO threshold is even lower than the reported value of 0.86 W in our recently published work, and the difference can be explained as follows. On the one hand, the Nd:YVO_4 crystal (0.5 at.% doped, 5 mm long) used in this experiment, in terms of lasing and thermally-conducting performances, is much better than that (1.0 at.% doped, 2 mm long) used in our previous work. On the other, as the OPO pump scheme employed here is a passively Q-switched one, the cavity configuration becomes more compact, and the round-trip and inserting losses are consequently reduced. It is seen in Fig. 3 that the signal average power increases linearly except for the case of $T_0 = 60\%$, and the corresponding critical diode pump power is about 3.3 W which is in good agreement with the theoretical estimations. As discussed in Section 3, the parametric power fall-off can be attributed to the conjunct TLE in the Nd:YVO_4 and Cr:YAG crystals. In other words, when the TLE is much serious, the laser cavity becomes unstable, leading to the degradation of the fundamental intensity. Simultaneously, the intracavity loss is enhanced due to the reduction of the intensity-dependent transmission of the Cr:YAG saturable absorbers, which eventually results in the fast decrease of the average output at 1573 nm. At the incident diode pump power of 4 W, we obtained a maximum signal average power of 358 mW, corresponding to the fundamental-to-signal and diode-to-signal conversion efficiencies of 27.5% and 9%, respectively.

The temporal behaviors of the signal and fundamental pulses were detected by a fast InGaAs photodiode and recorded by a LeCroy 9361 C Dual 300 MHz oscilloscope. Fig. 4 depicts the synchronous temporal profiles of the pulses at 1064 and 1573 nm after the OPO began to oscillate. From it, one can see clearly the buildup mechanism of the signal pulses and also the correlation dynamics between the laser and the OPO, which can be interpreted in the following way. At the first stage, after the saturable absorber was bleached, the intracavity fundamental intensity went up with the diode pump level. When the intensity is sufficiently high to exceed the OPO threshold, the parametric converting process started up, leading to the fast buildup of the signal pulses and simultaneously the rapid decrease of the fundamental field. In order to visually and well understand the energy conversion from the fundamental field to the signal one, we observed and recorded the pulse transforming process from 1064 to 1573 nm by slightly altering the pump level around the OPO threshold, which is plotted in Fig. 5. In this figure, graph (a) is the pulse shape of 1064 nm before the parametric oscillation. Fig. 5b and c reveals that the signal pulses, at the expense of the fundamental field, began to grow up from the quantum noise. As Fig. 5d shows, the output pulses at 1573 nm eventually come into being, and the fundamental field was almost completely attenuated. It can also be seen that during the transforming process, the fundamental pulses were compressed by several orders, which was attributed to the excellent cavity-dumping property of the IOPO. In the experiment, the typical pulse duration of 1064 nm was about 20 ns, while that of 1573 nm was only in the range of 1.6–2.2 ns at different pump levels. The detected signal pulse repetition rate varies from 5 to 41 kHz on the whole pump scope and with different Cr:YAG saturable absorb-

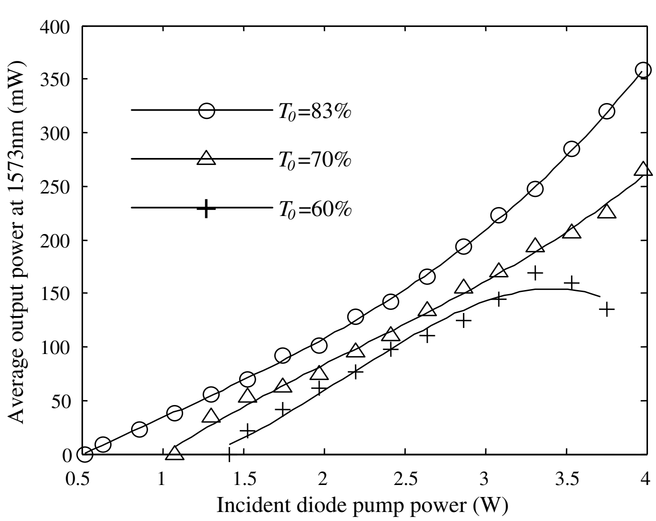

Fig. 3. The average output power at 1573 nm as a function of the incident diode pump power, and with different Cr:YAG saturable absorbers.

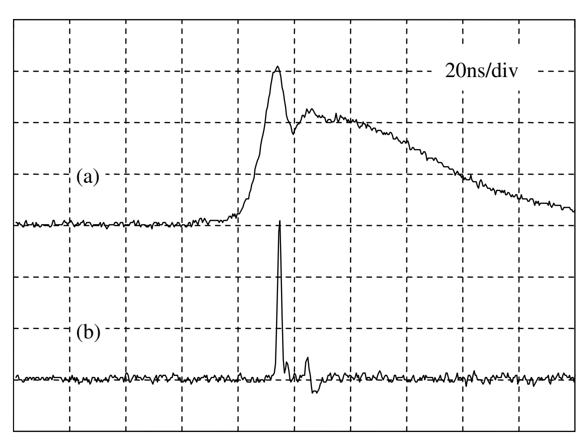

Fig. 4. Synchronous temporal shapes of the fundamental (a) and signal (b) pulses after the OPO begins to oscillate.

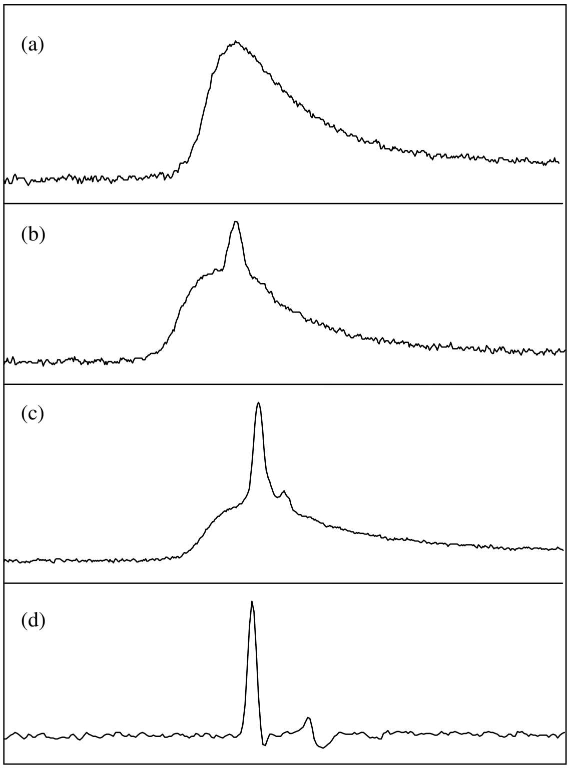

Fig. 5. Pulse transforming process from 1064 to 1573 nm around the OPO oscillation threshold. (a) Pulse profile of 1064 nm before the OPO oscillation. (b and c) Pulse shapes in the transition. (d) Temporal profile of the signal pulses.

ers. Pulse shortening mechanism inevitably leads to high peak power output at 1573 nm which is depicted in Fig. 6. It is seen that at the incident diode pump power of 4 W and signal pulse repetition rate of 7.5 kHz, we obtained a maximum peak power of 12.5 kW using the saturable absorber with $T_0 = 60\%$.

Multipulsing phenomenon of the IOPO, which was caused by the relatively too high signal reflectivity of

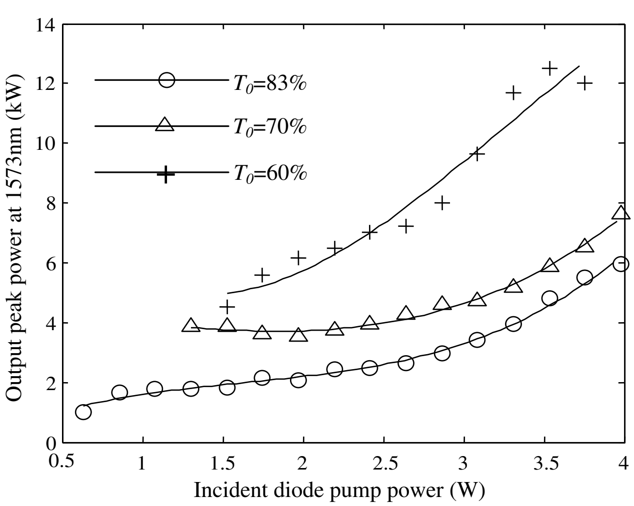

Fig. 6. The output peak power of 1573 nm as a function of the incident diode pump power using different Cr:YAG saturable absorbers.

the output coupler, was observed in the experiment and was illustrated in Figs. 4 and 5d. Single-pulse operation could be achieved through choosing an ideal output coupler with appropriate reflectivity at the signal wave [18]. In addition, we also found that owing to the wide absorption bandwidth of Nd:YVO_4, the cooling impact of the diode laser on the signal output was negligible. However, the cooling of KTP had a severe influence on the parametric conversion efficiency. It can be explained that during the operation of the IOPO, the phase-matching condition was well satisfied, and a stable thermal distribution was established in the KTP crystal. When we further cooled the nonlinear crystal, the thermal distribution was broken and the heat gradient was enhanced, resulting in the local non-uniformity of the refractive index of the KTP crystal. Therefore, the phase-matching was destroyed and ultimately led to the degradation of the signal output.

5. Conclusions

In summary, the operation of a compact low threshold (0.52 W) Cr:YAG passively Q-switched IOPO at 1573 nm has been demonstrated. Based on the ABCD matrix approach, the thermal lens effect of the Cr:YAG saturable absorber, which we consider a key factor that affects the signal output, has been discussed, holding good agreement with the experimental results. Efficient pulse shortening mechanism and cavity-dumping characteristic of the IOPO have resulted in high peak power output (12.5 kW) at 1573 nm. It has been experimentally revealed that, in order to improve the OPO conversion efficiency, the thermal lens effect of the saturable absorber must be elaborately treated, and the thermal stabilization in the KTP crystal should also be well maintained.

References

[1] A. Dubois, S. Victori, T. Lepine, P. Georges, A. Brun, Appl. Phys. B 67 (1998) 181.
[2] R. Dabu, A. Stratan, C. Fenic, C. Luculescu, L. Muscalu, Opt. Eng. 40 (2001) 455.
[3] Xingyu Zhang, Shenzhi Zhao, Qingpu Wang, Qidi Zhang, Lianke Sun, Shaojun Zhang, IEEE J. Quantum Electron. 33 (1997) 2286.
[4] Jingang Liu, Dalwoo Kim, IEEE J. Quantum Electron. 35 (1999) 1724.
[5] R.S. Conroy, C.F. Rae, G.J. Friel, M.H. Dunn, B.D. Sinclair, Opt. Lett. 23 (1998) 1348.
[6] Y.F. Chen, S.W. Chen, Y.C. Chen, Y.P. Lan, S.W. Tsai, Appl. Phys. B 77 (2003) 493.
[7] Y.F. Chen, Y.C. Chen, S.W. Chen, Y.P. Lan, Opt. Commun. 234 (2004) 337.
[8] W. Zendzian, J.K. Jabczynski, P. Wachulak, J. Kwiatkowski, Appl. Phys. B 80 (2005) 329.
[9] Jieguang Miao, Huiming Tan, Huikun Bian, Baoshan Wang, Jiying Peng, Opt. Commun. 265 (2006) 349.
[10] Th. Graf, E. Wyss, M. Roth, H.P. Weber, Opt. Commun. 190 (2001) 327.
[11] Feng Song, Chaobo Zhang, Xin Ding, Jingjun Xu, Guangyin Zhang, Appl. Phys. Lett. 81 (2002) 2145.

[12] Jie Song, Cheng Li, Ken-ichi Ueda, Opt. Commun. 177 (2000) 307.
[13] M.E. Innocenzi, H.T. Yura, C.L. Fincher, R.A. Fields, Appl. Phys. Lett. 56 (1990) 1831.
[14] Baida Lü, Laser Optics, third ed., Higher Education Press, Beijing, 2003 (in Chinese).
[15] Yung-Fu Chen, Hui-Jean Kuo, Opt. Lett. 23 (1998) 846.
[16] T.Y. Fan, IEEE J. Quantum Electron. 29 (1993) 1457.
[17] Y.P. Lan, Y.F. Chen, S.C. Wang, Appl. Phys. B 71 (2000) 27.
[18] Guohua Xiao, Michael Bass, Madhu Acharekar, IEEE J. Quantum Electron. 34 (1998) 2241.